Chemical Engineering Journal 162 (2010) 515–520

Contents lists available at ScienceDirect

Chemical Engineering Journal

journal homepage: www.elsevier.com/locate/cej

Effect of temperature and concentration on reduction and oxidation of NO over SOFC cathode of Cu-added (LaSr)(CoFe)O_3-(Ce,Gd)O_{2-x}

Ta-Jen Huang*, Chien-Liang Chou

Department of Chemical Engineering, National Tsing Hua University, Hsinchu 300, Taiwan, ROC

ARTICLE INFO

Article history:
Received 12 April 2010
Received in revised form 24 May 2010
Accepted 26 May 2010

Keywords:
Electrochemical NO reduction
NO_2 formation
Activation energy
Temperature
Concentration
Solid oxide fuel cell

ABSTRACT

A solid oxide fuel cell (SOFC) unit is constructed with Ni-(Ce,Gd)O_{2-x} as the anode, yttria-stabilized zirconia as the supporting electrolyte, and Cu-added (LaSr)(CoFe)O_3-(Ce,Gd)O_{2-x} as the cathode. Both reduction and oxidation of NO occur and are affected by the concentration of NO. Either reduction or oxidation of NO starts from NO adsorption. NO reduction to generate an electrical current has very much smaller activation energy than NO oxidation to form NO_2. With 4% O_2 and 1000 ppm NO, the NO_2 yield is relatively small and the temperature effect on NO reduction is positive. These are beneficial for the application of the process of DeNO_x by SOFC to NO abatement from the lean-burn engine exhausts.

1. Introduction

The control of nitrogen oxides (NO_x, NO plus NO_2) emission from industrial flue gas in stationary sources is traditionally performed by the selective catalytic reduction (SCR) process, in which NO_x in the flue gas reacts with ammonia to produce nitrogen and water [1]. This SCR process has to use a reducing gas, usually ammonia; however, the residual ammonia can pose a problem and needs additional treatment. Thus, the electrochemical NO reduction without a reducing gas has been studied extensively [2–7]. However, this process of electrochemical NO reduction is performed with applied current and the current efficiency is generally only a few percent; additionally, the reduction of O_2 occurs simultaneously to consume a substantial amount of the electrical current [7]. Therefore, electrochemical NO reduction with power generation via solid oxide fuel cells (SOFCs) should be an attractive process; this process has been shown to be feasible for NO_x removal [8–10]. Nevertheless, this process of DeNO_x by SOFC needs an anode fuel. However, the anode fuel is consumed only when the oxygen ion is transported to the anode to carry out the electrochemical oxidation to generate an electrical current—that is, the NO_x conversion contributes to power generation. Thus, DeNO_x by SOFC is very energy-efficient.

A process of DeNO_x by SOFC means that the SOFC operation is performed with the flue gas passing the cathode side; for the flue gas of the power plant or the nitric acid plant, the O_2 concentration is usually 4–6% and the NO concentration can be 0.1–0.5% or higher. Recently, the problem of CO_2 emission has become very critical. The lean-burn engines are promising to decrease the fuel consumption for automotive use and thus decrease the CO_2 emission. However, for NO_x abatement from the exhaust of the lean-burn engines, an efficient NO_x reduction at high oxygen concentrations is needed. In the lean-burn engine exhaust, the O_2 concentration is usually higher than 4% [11]. Additionally, temperature and NO concentration of the lean-burn engine exhaust may vary with varying operating conditions. Thus, the effects of temperature and concentration on electrochemical NO reduction via SOFCs should be interesting to be studied to see the feasibility of the process of DeNO_x by SOFC on exhaust emission control for lean-burn engines. Additionally, with the existence of NO in the presence of O_2, NO_2 may be formed via NO oxidation [9]. Therefore, the effects of temperature and concentration on NO oxidation should also be interesting to be studied.

(LaSr)(CoFe)O_3 (LSCF) is the well-known material for the cathode in intermediate temperature SOFCs, and adding gadolinia-doped ceria (GDC) into LSCF to make the LSCF-GDC composite as the cathode can increase the oxygen reduction activity of the cathode [12]. The addition of 50 vol.% GDC to LSCF has resulted in a decrease of the polarization resistance with a factor of about 10 compared to that of the LSCF cathode [13]. Thus, such LSCF-GDC composite will be used in this work. Additionally, Cu-added LSCF-GDC composite has been used as the SOFC cathode for DeNO_x by SOFC [9]. However, the effects of temperature and concentration on reduction and oxidation of NO over the SOFC cathode have not yet been studied; these effects will be investigated in this work.

---

* Corresponding author. Tel.: +886 3 5716260; fax: +886 3 5715408.
E-mail address: tjhuang@che.nthu.edu.tw (T.-J. Huang).

1385-8947/$ – see front matter © 2010 Elsevier B.V. All rights reserved.
doi:10.1016/j.cej.2010.05.053

In this work, the current–voltage measurement and the fixed-voltage test were performed in an SOFC unit cell with Cu-added LSCF-GDC cathode as well as cathode gases with various NO concentrations at 800–900 °C. The results show that NO reduction to generate an electrical current has very much smaller activation energy than NO oxidation to form NO_2. This is beneficial for the application of the process of $DeNO_x$ by SOFC to NO abatement from the lean-burn engine exhausts.

2. Experimental

2.1. Preparation of LSCF and GDC and Cu addition

LSCF was prepared by the glycine-nitrate process with a composition of $La_{0.58}Sr_{0.4}Co_{0.2}Fe_{0.8}O_{3-\delta}$. The details of the method have been described elsewhere [10]. The LSCF powders were calcined by heating in air at a rate of 5 °C min^{-1} to 500 °C and held for 2 h, then to 900 °C and held for 4 h, and then slowly cooled down to room temperature.

GDC was prepared by the co-precipitation method with a composition of $(GdO_{1.5})_{0.1}(CeO_2)_{0.9}$. The details of the method have been described elsewhere [14]. The GDC powders were calcined by heating in air at a rate of 5 °C min^{-1} to 900 °C and held for 4 h before cooling down.

The LSCF-GDC composite was prepared by mixing the above-prepared LSCF and GDC powders at LSCF:GDC = 100:50 in weight and thus designated as 100LSCF-50GDC. The mixture was ground for 24 h, then calcined by heating in air at a rate of 5 °C min^{-1} to 500 °C and held for 2 h, and then to 900 °C, held for 10 h before cooling down.

The Cu addition to 100LSCF-50GDC powders was done by impregnation. The Cu cation solution was prepared by dissolving $Cu(NO_3)_2{\cdot}3H_2O$ (Showa, Japan) in de-ionized water. After drying, the powders were calcined by heating in air at a rate of 5 °C min^{-1} to 900 °C and held for 4 h before cooling down. The Cu loading was 1 wt.% in terms of the weight of LSCF.

2.2. Construction of SOFC unit cell

The commercial yttria-stabilized zirconia (YSZ) tape (Jiuhow, Taiwan) was employed to make an electrolyte-supported SOFC cell. A disk of 1.8 cm in diameter was cut from the YSZ tape. One side of the disk was spin-coated with the paste of Ni-GDC as the anode, being composed of 60 wt.% Ni in terms of GDC, which has been shown to have an optimum anode performance [15]. The details of the preparation of the Ni-GDC paste have been described elsewhere [16]. The other side of the disk was spin-coated with a thin interlayer to enhance adhesion and then with Cu-added 100LSCF-50GDC as the cathode. The thus-prepared SOFC unit cell has an anode-layer thickness of 25 μm, an electrolyte-layer thickness of 156 μm, an interlayer thickness of 5 μm, a cathode-layer thickness of 20 μm, and a cathode area of 1.1 cm^2.

2.3. Current–voltage measurement

The measurement of current–voltage curve was performed at 800 °C with pure hydrogen flowing on the anode side and various gas mixtures, all balanced by argon, on the cathode side. The flow rates of various components in the gaseous mixtures were measured by mass flow meters, respectively, before entering into a mixer. The overall flow rate was 150 ml/min and that on the anode side was the same as that on the cathode side. The overall flow rate was measured by a gas bubble meter at the outlet of the experimental setup. The voltage was varied by an adjustable resister, and both the voltage and the current were measured by a Multimeter (TES 2730).

Table 1
Variation of open circuit voltage and maximum power density with inlet NO concentration (with 4% O_2) at 800 °C.

Inlet NO concentration (ppm)	Open circuit voltage (V)	Maximum power density[a] (mW cm^{-2})
1000	1.136	34.64
3000	1.136	34.95
5000	1.134	35.15

[a] Obtained via data from the current–voltage measurements.

2.4. Fixed-voltage test

The fixed-voltage tests were performed at 800–900 °C with the operating voltage kept constant at 0.55 V. The anode gas was pure hydrogen. The inlet cathode gas was a mixture of 4% O_2 and NO, balanced in argon, with the NO concentration designated in the figure and table legends. The overall flow rate was always 150 ml/min.

The tests were conducted with introducing a designated gas mixture to the cathode side of the SOFC unit cell. After a steady state was obtained for over 120 min, the NO concentration was increased. After the test of 1000–5000 ppm NO at the same temperature, the temperature was increased to a higher one as designated in the figure. Throughout the test, the electrical current, the voltage, and the outlet gas compositions were always measured. The NO and NO_2 contents in the outlet cathode gas were measured by NO and NO_2 analyzers (NGA 2000, Emerson, Germany), respectively.

3. Results and discussion

3.1. Effect of temperature on reduction and oxidation of NO

Table 1 shows that the open circuit voltage with cathode gases of 4% O_2 plus 1000–5000 ppm NO is close to the theoretical value; this indicates that there should be no leakage in the SOFC setup of this work. Additionally, the maximum power density increases with increasing NO concentration; this indicates the generation of an additional electrical current due to the presence of NO and thus confirms the occurrence of electrochemical NO reduction—that is, the occurrence of NO dissociation to produce the adsorbed N and O species:

$$NO \rightarrow N_{ads} + O_{ads} \quad (1)$$

Followed by the charge transfer reaction to form the oxygen ion:

$$O_{ads} + 2e^{-} \rightarrow O^{2-} \quad (2)$$

Notably, electrochemical NO reduction is completed and generates an electrical current only after the oxygen ion produced in reaction (2) has been transported to the anode via the oxygen-ion conducting electrolyte and consumed by electrochemical oxidation with the anode-side fuel.

Fig. 1 shows the steady state profiles of outlet NO and NO_2 concentrations with inlet NO concentration of 1000 ppm in 4% O_2 during the fixed-voltage tests. Notably, the vertical lines between these steady states as shown in Fig. 1 and similar figures latter are drawn by the drawing software and do not indicate any actual behavior. As the temperature increases from 800 to 900 °C, Fig. 1A shows that the outlet NO concentration decreases, indicating an increase of the NO consumption rate; Fig. 1B shows that the outlet NO_2 concentration increases, indicating an increase of the NO_2 formation rate. The formation of NO_2 indicates the occurrence of NO oxidation:

$$NO + O_{ads} \rightarrow NO_2 \quad (3)$$

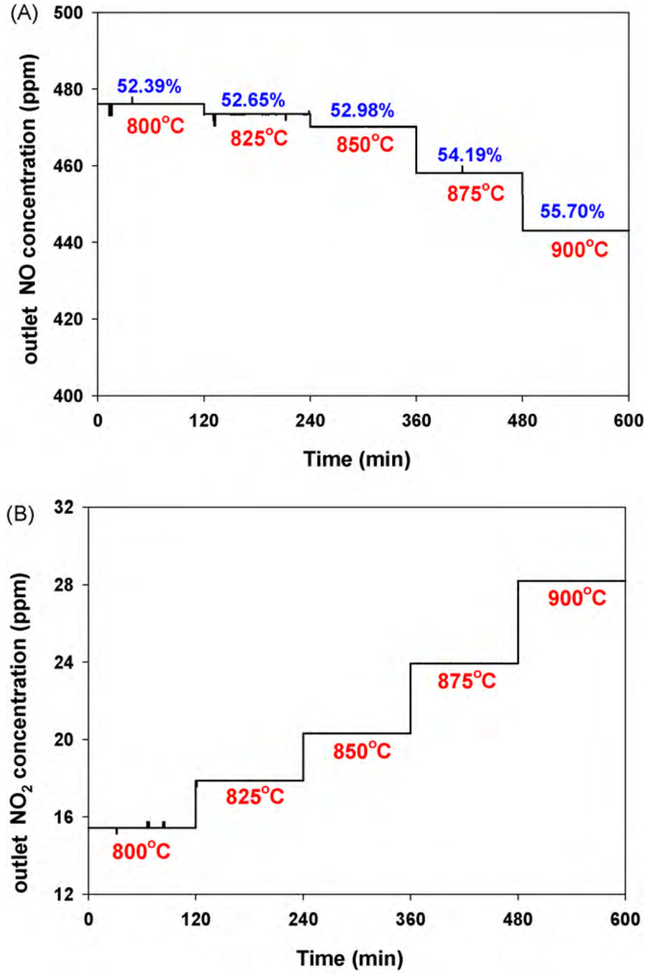

Fig. 1. Variations of (A) outlet NO concentration and (B) outlet NO_2 concentration with temperature. 4% O_2 + 1000 ppm NO inlet. NO conversion is indicated in blue above the data line.

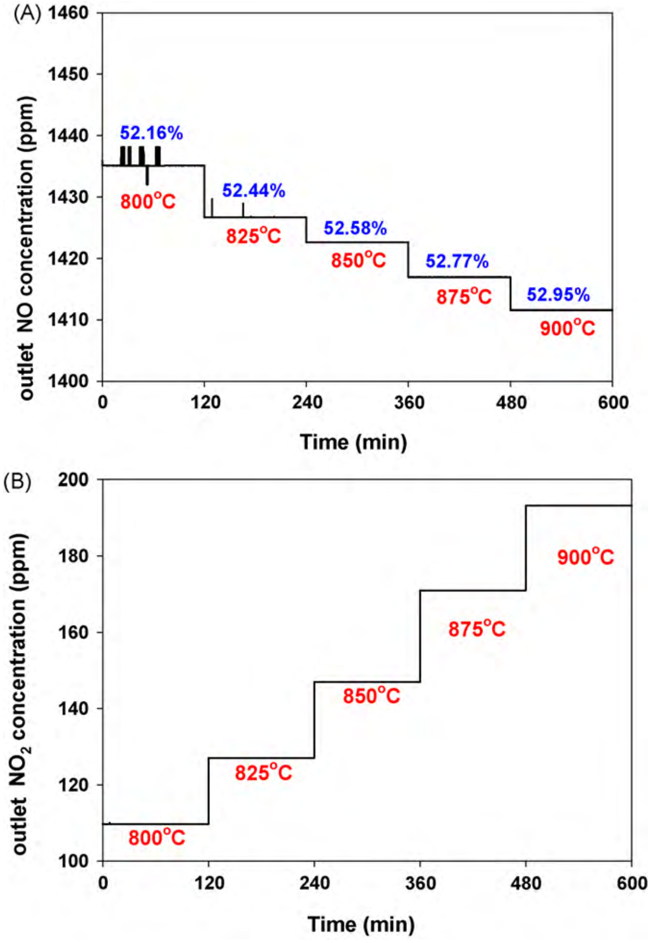

Fig. 2. Variations of (A) outlet NO concentration and (B) outlet NO_2 concentration with temperature. 4% O_2 + 3000 ppm NO inlet. NO conversion is indicated in blue above the data line.

Thus, the conversion of NO is due to both reduction and oxidation of NO—that is, NO consumption rate equals the sum of NO reduction rate and NO oxidation rate. Since NO oxidation forms NO_2, NO oxidation rate equals NO_2 formation rate. Therefore,

$$\text{NO reduction rate} = \text{NO comsumption rate} - \text{NO}_2\ \text{formation rate} \tag{4}$$

Notably, nitrous oxide (N_2O) has been considered to be an intermediate of electrochemical NO reduction [17]. However, with Cu as a catalytic agent over the cathode of an SOFC operating at 800 °C and higher temperature as in this work, the formation of N_2O can be negligible since Cu is an effective catalyst for the decomposition of N_2O to N_2 at 95 °C [18]; additionally, N_2O is not stable above 500 °C and quantitatively decomposed in the gas phase.

When the temperature increases from 800 to 900 °C, Fig. 2A and B show a decrease of the outlet NO concentration and an increase of the outlet NO_2 concentration, respectively, with inlet NO concentration of 3000 ppm; Fig. 3A and B show a decrease of the outlet NO concentration and an increase of the outlet NO_2 concentration, respectively, with inlet NO concentration of 5000 ppm. Table 2 presents the calculated NO conversion and the measured current density. As the temperature increases from 800 to 900 °C, both the NO conversion and the current density increase. However, the extent of increase of the NO conversion with increasing temperature is much smaller than that of the current density. This indicates that the increase of the current density is mostly due to oxygen reduction, that is, O_2 dissociation:

$$O_2 \rightarrow 2O_{ads} \tag{5}$$

followed by the charge transfer reaction (2); this is reasonable with a cathode gas containing 4% (40,000 ppm) O_2 and only 1000–5000 ppm NO. Notably, the transport of the O species from the cathode to the anode via the oxygen-ion conducting electrolyte generates an electrical current, indiscriminating the source of the O species.

When the temperature increases from 800 to 900 °C, Table 2 shows that both the NO reduction rate and the NO_2 formation (NO oxidation) rate increase with inlet NO concentration of 1000 ppm—that is, both the rates of reduction and oxidation of NO increase with increasing temperature. Notably, since NO oxidation is exothermic, its equilibrium conversion should decrease with increasing temperature if only reduction and oxidation of NO occur. However, when a large amount of oxygen presents, since the electrochemical oxidation over the SOFC anode needs a much larger amount of O species than being able to be supplied by NO dissociation, these O species are mostly supplied by oxygen via reaction (5); consequently, the possibility for NO oxidation becomes much higher than that when the O species comes only via NO dissociation. Thus, with increasing temperature, since the rate of electrochemical oxidation over the SOFC anode increases, the rate of NO oxidation over the SOFC cathode can increase. When the inlet NO concentration increases to 3000 or 5000 ppm, the NO oxidation rate also increases with increasing temperature but the

NO reduction rate decreases. This indicates an effect of NO concentration on its reduction.

Table 2 also shows that the NO_2 yield always increases with increasing temperature. However, at a same temperature, the NO_2 yield increases with increasing NO concentration from 1000 to 3000 ppm but decreases with further increasing NO concentration to 5000 ppm. This indicates an effect of NO concentration on the NO_2 yield. Since the NO_2 yield is associated with both the rates of reduction and oxidation of NO, there exists an effect of concentration on reduction and oxidation of NO.

3.2. *Effect of concentration on reduction and oxidation of NO*

Table 2 also shows that, when the inlet NO concentration increases from 1000 to 5000 ppm at the same temperature, the current density increases. This indicates that electrochemical NO reduction occurs to contribute to the generation of an electrical current. With increasing NO concentration, both the rates of NO reduction and NO_2 formation (NO oxidation) increase, in accordance with reactions (1) and (3); however, the NO conversion decreases. This indicates that NO needs to be adsorbed first:

$$NO_{gas} \rightarrow NO_{ads} \tag{6}$$

When the amount of the active sites for NO adsorption is limited, the NO reactions cannot take full advantage of the beneficial effect of increasing concentration to increase their rates. This can decrease the NO conversion. Additionally, the extent of increase of the NO conversion with increasing temperature decreases with increasing NO concentration. This is also due to a limited amount of the active sites for NO adsorption and thus the NO reactions cannot take full advantage of the beneficial effect of increasing temperature to increase their rates. These confirm that the reactions start from reaction (6)—that is, either reduction or oxidation of NO starts from the adsorption of NO. Therefore, reaction (1) should consist of reaction (6) and the dissociation of adsorbed NO:

$$NO_{ads} \rightarrow N_{ads} + O_{ads} \tag{1'}$$

Additionally, reaction (3) should consist of reaction (6) and the oxidation of adsorbed NO:

$$NO_{ads} + O_{ads} \rightarrow NO_2 \tag{3'}$$

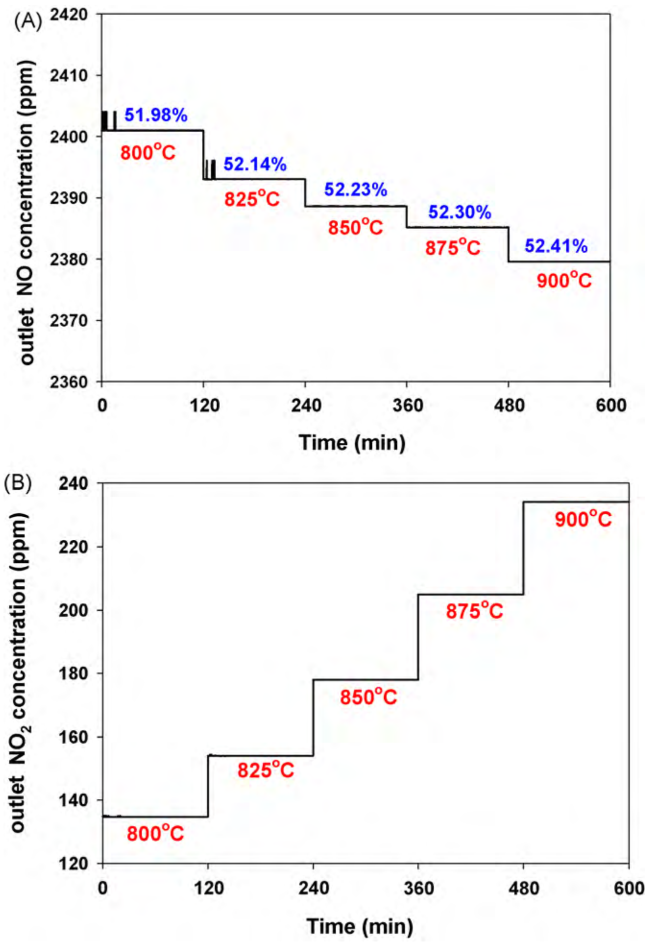

Fig. 3. Variations of (A) outlet NO concentration and (B) outlet NO_2 concentration with temperature. 4% O_2 + 5000 ppm NO inlet. NO conversion is indicated in blue above the data line.

Table 2
Variation of steady-state NO consumption rate, NO conversion, NO reduction rate, NO_2 formation rate, NO_2 yield and current density with temperature and inlet NO concentration.

Temperature (°C)	NO consumption rate[a]	NO conversion (%)	NO reduction rate[a,b]	NO_2 formation rate[a]	NO_2 yield[c] (%)	Current density[d] (mA cm^{-2})
Inlet 1000 ppm NO						
800	0.836	52.39	0.811	0.0246	2.94	62.96
825	0.841	52.65	0.812	0.0285	3.39	65.67
850	0.846	52.98	0.814	0.0324	3.83	73.95
875	0.865	54.19	0.827	0.0382	4.42	75.32
900	0.889	55.69	0.844	0.0450	5.06	77.05
Inlet 3000 ppm NO						
800	2.498	52.16	2.323	0.175	7.01	63.50
825	2.512	52.44	2.309	0.203	8.08	67.59
850	2.518	52.58	2.283	0.235	9.33	74.51
875	2.527	52.77	2.254	0.273	10.8	76.41
900	2.536	52.95	2.228	0.308	12.1	78.61
Inlet 5000 ppm NO						
800	4.149	51.98	3.934	0.215	5.18	63.88
825	4.162	52.14	3.916	0.246	5.91	68.29
850	4.169	52.23	3.885	0.284	6.81	74.95
875	4.174	52.30	3.847	0.327	7.83	76.57
900	4.183	52.41	3.809	0.374	8.94	78.85

[a] Rate in μmol cm^{-2} min^{-1}.
[b] NO reduction rate = NO consumption rate – NO_2 formation rate.
[c] NO_2 yield = [(amount of NO_2 formed)/(amount of NO converted)] × 100%.
[d] Obtained from the fixed-voltage test at 0.55 V.

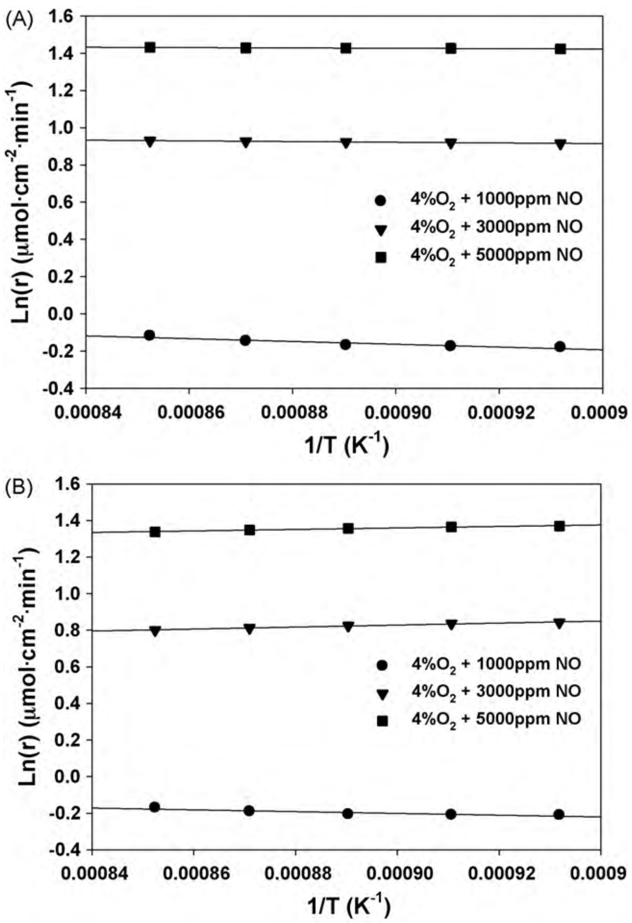

Fig. 4. Arrhenius plots of (A) NO consumption and (B) NO reduction with 4% O_2 and various NO contents.

with the adsorbed O species coming from either reaction (1′) or (5). Notably, reaction (6) should not be the rate-determining step for NO reactions if the activation energy for reduction and oxidation of NO is different; this is because, if reaction (6) is the rate-determining step for both reduction and oxidation of NO, both rates of reduction and oxidation of NO should be the same according to the definition of "rate-determining step" and thus the activation energy should be the same.

3.3. Activation energy for NO reduction and NO_2 formation

Fig. 4 shows the Arrhenius plots of the rates of consumption and reduction of NO with NO concentration of 1000–5000 ppm, respectively. Both Fig. 4A and B clearly show that it should not be proper to put all the data of 1000–5000 ppm NO together to draw a unified plot. Thus, the Arrhenius plot should depend on the NO concentration as shown—that is, the activation energy depends on the concentration of NO. The calculated activation energies are presented in Table 3. Notably, since the NO consumption rate equals the sum of the NO reduction rate and the NO oxidation rate, the activation energy for NO consumption may not be associated with a rate-determining step but can show the temperature dependence of overall NO conversion. With the NO concentration of 3000 or 5000 ppm, the negative value of the activation energy for NO reduction is also only to show the negative temperature dependence—that is, the rate of NO reduction decreases with increasing temperature. Notably, also, during electrochemical NO reduction with an applied current, the selectivity for NO reduction decreases with increasing temperature [7]. Nevertheless, the NO concentration in the lean-burn engine exhausts is usually smaller than 1000 ppm [11]; thus, the relatively small activation energy and the positive temperature dependence for reduction of 1000 ppm NO should be beneficial for the application of the process of $DeNO_x$ by SOFC to NO abatement from the lean-burn engine exhausts.

Table 3
Variation of activation energies of NO consumption, NO reduction and NO_2 formation (NO oxidation) with inlet NO concentration.

Inlet NO concentration (ppm)	NO consumption (kJ/mol)	NO reduction (kJ/mol)	NO_2 formation (kJ/mol)
1000	6.27	4.06	62.65
3000	1.51	(−4.50)[a]	59.85
5000	0.81	(−3.44)[a]	58.27

[a] Presented to show the temperature dependence.

Fig. 5 shows the Arrhenius plots of the rates of NO_2 formation (NO oxidation) and it also shows that the Arrhenius plot should depend on the NO concentration. Table 3 shows that the activation energy for NO_2 formation is very much larger than that for NO reduction. Notably, over the Cu-added LSCF-GDC cathode of this work, the activation energy for NO_2 formation via NO oxidation is around 60 kJ/mol, which is smaller than that of around 80 kJ/mol for NO oxidation over Pt [19]. This indicates that NO reduction via reaction (1′) is very much faster than NO_2 formation via reaction (3′)—that is, removing the O species from NO is much easier than adding it onto NO. This may be explained by the consideration that the reaction of the O species over the SOFC cathode is a process of electrochemical reduction, at least during power generation. With a relatively large O_2 concentration, the current density can be large; this means that the rate of electrochemical reduction of the O species is large. Notably, also, electrochemical reduction of the O species occurs indiscriminating the source of the O species. A large current density means a fast removal of the O species produced by reaction (1′) and thus the rate of reaction (1′) can be large. This is in agreement with the observation that increasing O_2 concentration can increase the NO conversion [9].

On the other hand, although the relatively large O_2 concentration can also result in the oxidation of NO to form NO_2, the process of adding the O species onto NO is against that of electrochemical reduction during power generation—that is, the O species should be transported from the cathode to the anode. Therefore, the rate of NO oxidation (NO_2 formation) can be much smaller than that of NO reduction. Additionally, Fig. 1B shows that the formed NO_2 with 1000 ppm NO inlet is smaller than 30 ppm; this amount of NO_2 can be completely converted to NO in a subsequent SOFC unit since

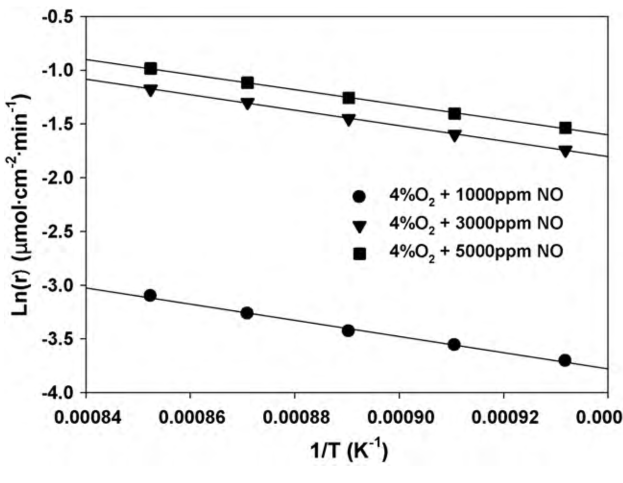

Fig. 5. Arrhenius plots of NO_2 formation with 4% O_2 and various NO contents.

100% NO_2 conversion has been observed with 4% O_2 and 150 ppm NO_2 inlet [9]. This is beneficial for the application of the process of $DeNO_x$ by SOFC with power generation to remove NO from the lean-burn engine exhausts.

Table 3 also shows that either the activation energy of NO consumption or that of NO_2 formation decreases with increasing NO concentration. This may be attributed to a competition of NO with O_2 for adsorption onto the active site. Notably, NO consumption consists of both reduction and oxidation of NO and either reduction or oxidation of NO starts with the adsorption of NO. When the NO concentration increases, its ability to compete with O_2 for adsorption onto the active site can increase; this may result in a decrease of the activation energy. This decrease of the activation energy may be associated with the effect of NO concentration on reduction and oxidation of NO. However, this needs the determination of the rate-determining step for either reduction or oxidation of NO and further studies are needed for clarification.

4. Conclusions

(1) The conversion of NO is due to both reduction and oxidation of NO.
(2) NO concentration has an effect on either reduction or oxidation of NO.
(3) Either reduction or oxidation of NO starts from the adsorption of NO.
(4) With 4% O_2 and 1000 ppm NO, the NO_2 yield is relatively small and the temperature effect on NO reduction is positive.
(5) NO reduction to generate an electrical current has very much smaller activation energy than NO oxidation to form NO_2.

References

[1] H. Bosch, F. Janssen, Formation and control of nitrogen oxides, Catal. Today 2 (1988) 369–379.

[2] T. Hibino, K. Ushiki, Y. Kuwahara, M. Mizuno, Electrochemical removal of NO in the presence of excess O_2, H_2O and CO_2 using Sm_2O_3-doped CeO_2 as a solid electrolyte, Solid State Ionics 89 (1996) 13–16.

[3] K.K. Hansen, E.M. Skou, H. Christensen, Perovskites as cathodes for nitric oxide reduction, J. Electrochem. Soc. 147 (2000) 2007–2012.

[4] S. Kim, G.L. Haller, Solid electrolyte aided studies of NO–CO reaction on Pd, Solid State Ionics 136–137 (2000) 693–697.

[5] A.C.A. de Vooys, M.T.M. Koper, R.A. van Santen, J.A.R. van Veen, Mechanistic study on the electrocatalytic reduction of nitric oxide on transition-metal electrodes, J. Catal. 202 (2001) 387–394.

[6] S. Bredikhin, K. Maeda, M. Awano, Low current density electrochemical cell for NO decomposition, Solid State Ionics 152–153 (2002) 727–733.

[7] K. Kammer, Electrochemical $DeNO_x$ in solid electrolyte cells—an overview, Appl. Catal. B: Environ. 58 (2005) 33–39.

[8] T.J. Huang, C.L. Chou, Feasibility of simultaneous NO reduction and electricity generation in SOFCs with V_2O_5 or Cu added LSCF-GDC cathodes, Electrochem. Commun. 11 (2009) 477–480.

[9] T.J. Huang, C.L. Chou, Electrochemical NO_x reduction with power generation in solid oxide fuel cells with Cu-added $(LaSr)(CoFe)O_3$-$(Ce,Gd)O_{2-x}$ cathode, J. Electrochem. Soc. 157 (2010) P28–P34.

[10] T.J. Huang, C.L. Chou, Effect of voltage and temperature on NO removal with power generation in SOFC with V_2O_5-added LSCF-GDC cathode, Chem. Eng. J. 160 (2010) 79–84.

[11] L. Li, J. Chen, S. Zhang, N. Guan, T. Wang, S. Liu, Selective catalytic reduction of nitrogen oxides from exhaust of lean burn engine over in situ synthesized monolithic Cu–TS-1/cordierite, Catal. Today 90 (2004) 207–213.

[12] T.J. Huang, X.D. Shen, C.L. Chou, Characterization of Cu, Ag and Pt added $La_{0.6}Sr_{0.4}Co_{0.2}Fe_{0.8}O_{3-\delta}$ and gadolinia-doped ceria as solid oxide fuel cell electrodes by temperature-programmed techniques, J. Power Sources 187 (2009) 348–355.

[13] E.P. Murray, M.J. Sever, S.A. Barnett, Electrochemical performance of $(La,Sr)(Co,Fe)O_3$–$(Ce,Gd)O_3$ composite cathodes, Solid State Ionics 148 (2002) 27–34.

[14] T.J. Huang, C.H. Wang, Factors in forming CO and CO_2 over cermet of Ni-gadolinia-doped ceria with relation to direct methane SOFCs, J. Power Sources 163 (2006) 309–315.

[15] J.B. Wang, J.C. Jang, T.J. Huang, Study of Ni-samaria-doped ceria anode for direct oxidation of methane in solid oxide fuel cells, J. Power Sources 122 (2003) 122–131.

[16] T.J. Huang, M.C. Huang, Electrochemical promotion of bulk lattice-oxygen extraction for syngas generation over Ni-GDC anodes in direct-methane SOFCs, Chem. Eng. J. 135 (2008) 216–223.

[17] T. Hibino, T. Inoue, M. Sano, Electrochemical reduction of NO by alternating current electrolysis using yttria-stabilized zirconia as the solid electrolyte: part II. Modification of Pd electrode by coating with Rh, Solid State Ionics 130 (2000) 31–39.

[18] H.F. Chang, M.A. Saleque, W.S. Hsu, W.H. Lin, Effect of acidity and copper surface area of the Formula Not Shown Formula Not Shown catalyst prepared by electroless plating procedure on dehydrogenation reactions, J. Mol. Catal. 94 (1994) 233–242.

[19] S.S. Mulla, N. Chen, L. Cumaranatunge, G.E. Blau, D.Y. Zemlyanov, W.N. Delgass, W.S. Epling, F.H. Ribeiro, Reaction of NO and O_2 to NO_2 on Pt: kinetics and catalyst deactivation, J. Catal. 241 (2006) 389–399.